

Interpretation of the Proton NMR Spectrum of Poly(vinylbutyral) by Two-Dimensional NMR

Martha D. Bruch* and Jo-Anne K. Bonesteel

E. I. du Pont de Nemours and Company, Polymer Products Department, E269, Wilmington, Delaware 19898. Received December 10, 1985

ABSTRACT: Poly(vinylbutyral) is a complex polymer formed from the condensation of poly(vinyl alcohol) and butyraldehyde. Two-dimensional ^{13}C - ^1H correlated spectroscopy is used in combination with distortionless enhancement by polarization transfer (DEPT) spectroscopy to make proton line assignments. These assignments are confirmed by homonuclear two-dimensional correlated spectroscopy (COSY). Furthermore, ^1H chemical shifts can be accurately measured from the COSY spectrum despite severe spectral overlap. Once the proton line assignments have been determined, homonuclear two-dimensional J -resolved spectroscopy is used to determine scalar coupling constants for some protons. Some variation of the coupling constants with stereosequences is observed. In addition, fine structure due to longer sequence sensitivity is observed in the J -resolved spectrum of poly(vinylbutyral).

Introduction

Proton NMR spectroscopy is potentially an extremely powerful technique for analysis of synthetic polymers since the chemical shifts and homonuclear coupling constants are sensitive to chain configuration and conformation, respectively. However, extensive overlap of resonances causes the proton spectra of complex polymer systems to be characterized by broad, ill-defined resonances in contrast to the well-defined multiplets characteristic of proton spectra of small biological and organic molecules. Consequently, traditional line assignment techniques such as spin decoupling generally cannot be used to assign lines in the proton spectra of synthetic polymers. Furthermore, scalar coupling constants cannot be measured easily from conventional spectra. All of these factors combine to make the proton spectrum of a complex polymer system extremely difficult to interpret.

Two-dimensional homonuclear correlated spectroscopy (COSY) and J -resolved spectroscopy have been applied extensively to the interpretation of proton spectra of biological macromolecules such as proteins,¹⁻⁷ antibiotics,⁸ peptides,⁹⁻¹³ nucleic acids,^{14,15} and oligosaccharides.¹⁶⁻¹⁸ However, applications of these techniques to the interpretation of proton spectra of synthetic polymers have been more limited. Homonuclear 2D J -resolved spectroscopy has been applied to the interpretation of proton spectra of poly(propylene oxide),¹⁹ poly(vinyl chloride),²⁰ and poly(vinyl alcohol).²¹ Two-dimensional COSY experiments have been applied to poly(vinyl alcohol)²² and poly(methyl methacrylate).²³ Cheng et al. have applied 2D ^{13}C - ^1H correlated spectroscopy to the interpretation of proton spectra of polyolefins.^{24,25}

We report the application of homonuclear 2D J -resolved, COSY, and ^{13}C - ^1H correlated spectroscopy to the interpretation of the proton spectrum of poly(vinylbutyral) (PVB). Poly(vinylbutyral) is a complex polymer resulting from the condensation reaction of butyraldehyde (BA) with poly(vinyl alcohol) (PVA). The butyraldehyde reacts with adjacent hydroxyl groups on PVA to form BA rings. The resultant polymer, PVB, is essentially a copolymer of BA rings and unreacted vinyl alcohol. Hence, this polymer exhibits both stereosequence and comonomer sequence microstructure. By combining several 2D techniques along with distortionless enhancement by polarization transfer (DEPT), one can make detailed line assignments in both the proton and carbon-13 spectra of this extremely complex polymer. Furthermore, some coupling constants are obtained from the 2D J -resolved spectrum.

Experimental Section

Materials. Poly(vinylbutyral) is made from the condensation reaction of poly(vinyl alcohol) with butyraldehyde. PVB was obtained from E. I. du Pont de Nemours and Co. All samples were dissolved in $\text{Me}_2\text{SO}-d_6$ which was purchased from Columbia Organic Chemicals and used without further purification. Wilmad 20- and 5-mm-diameter tubes were used for ^{13}C and ^1H NMR experiments, respectively.

NMR Methods. Distortionless enhancement by polarization transfer (DEPT) spectroscopy was performed to determine the multiplicity of each ^{13}C resonance. A standard pulse sequence,²⁶ shown in Figure 1, was employed. In this sequence, the preparation period is a relaxation delay to ensure that the protons are fully relaxed. The multiplicity is determined by varying the proton pulse, θ . When $\theta = 45^\circ$, all protonated signals are observed, but when $\theta = 90^\circ$, only methine carbon signals are observed. When $\theta = 135^\circ$, methine and methyl signals are positive, but methylene signals are negative. Signals corresponding to quaternary carbons have zero intensity for all values of θ .

Two-dimensional ^{13}C - ^1H correlated spectroscopy was performed by using the standard pulse sequence shown in Figure 2.²⁷ In this sequence, the preparation period ensures that the protons are fully relaxed. The first 90° proton pulse causes the protons to precess at their initial frequencies. The 180° ^{13}C pulse refocuses dephasing which has occurred due to ^{13}C - ^1H J -coupling. Consequently, the initial precession frequencies during t_1 depend only on the proton chemical shifts and homonuclear coupling constants. The delay time $\Delta_1 = 1/2J$ is necessary to allow the individual components of a ^1H - ^{13}C multiplet to dephase to the antiparallel alignment, which is optimal for polarization transfer. Polarization transfer between protons and directly attached ^{13}C nuclei is caused by the simultaneous ^1H and ^{13}C 90° pulses. The delay $\Delta_2 = 1/4J$ is necessary to ensure optimal detection, and the resultant ^{13}C FID is detected with proton decoupling during t_2 . The final frequencies reflect only the carbon chemical shifts corresponding to protonated carbons. The 2D ^{13}C - ^1H correlated spectrum maps each proton signal to the carbon-13 signal of the corresponding directly attached carbon.

Homonuclear 2D correlated spectroscopy (COSY) was performed by using the standard sequence $\text{RD}-90^\circ-t_1-90^\circ-t_2$.²⁸ The first 90° pulse causes each proton to precess at its initial frequency during t_1 . The second 90° pulse, or mixing pulse, causes magnetization exchange between protons which are J -coupled to each other, and the final frequency is detected. Those spins that do not exchange have a final frequency that is equal to the initial frequency. Hence, the COSY spectrum contains the normal spectrum along the diagonal given by $\omega_1 = \omega_2$. Those spins that do exchange due to J -coupling give rise to pairs of cross peaks or off-diagonal peaks connecting coupled protons. Hence, the COSY spectrum is a map of the complete homonuclear coupling network.

Homonuclear 2D J -resolved spectroscopy was performed by using the spin-echo pulse sequence²⁹ $\text{RD}-90^\circ-t_1/2-180^\circ-t_1/2-t_2$.

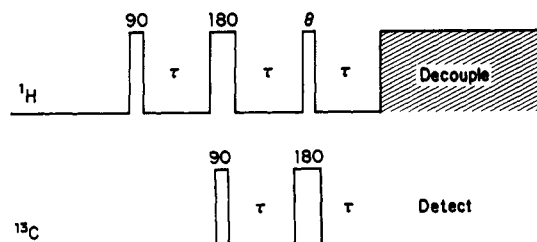


Figure 1. Pulse sequence for distortionless enhancement by polarization transfer (DEPT) spectroscopy. The third ¹H pulse is variable with $\theta = 45^\circ, 90^\circ$, and 135° . The delay time τ is set to $(2J_{^{13}\text{C}-^1\text{H}})^{-1}$.

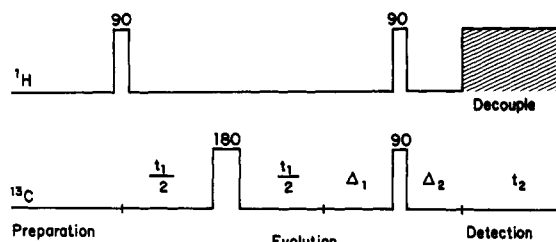


Figure 2. Pulse sequence for 2D ¹³C-¹H correlated spectroscopy. The delay times Δ_1 and Δ_2 are set to $(2J_{^{13}\text{C}-^1\text{H}})^{-1}$ and $(4J_{^{13}\text{C}-^1\text{H}})^{-1}$, respectively.

The 90° pulse flips the net magnetization vector into the xy plane, and the individual components dephase during the first interval $t_1/2$ due to differences in chemical shifts and coupling constants. The 180° pulse refocuses the spin isochromats that have dephased due to chemical shift differences but not those that have dephased due to J -coupling. The resultant signal is detected after a refocusing interval of length $t_1/2$. The initial frequency during t_1 reflects only J -coupling, whereas the final frequency reflects both chemical shifts and J -coupling. After a "tilt" of 45° ,³⁰ the ω_2 -axis reflects only chemical shifts, and ω_1 -axis reflects only J -coupling. Hence, overlapped multiplets can be resolved.

Proton spin-lattice relaxation times were estimated from an inversion-recovery sequence given by RD- 180° - τ - 90° -detect. The longest T_1 was 2 s.

NMR Measurements. All spectra were recorded on a Bruker AM-300 spectrometer equipped with an Aspect 3000 computer. Chemical shifts were referenced to $\text{Me}_2\text{SO}-d_6$ (¹³C frequency at 39.5 ppm, ¹H frequency of 2.49 ppm). All pulse sequences include a 16-cycle phase cycling routine. Each 2D spectrum was zero-filled in both dimensions prior to Fourier transformation, and the absolute value (magnitude) spectrum was calculated. A sine-bell or phase-shifted sine-bell filtering function was used in both dimensions prior to Fourier transformation to improve resolution. Homonuclear 2D spectra were all symmetrized to eliminate the bands of "t₁ noise" arising from spectrometer instabilities during the extended acquisition times associated with those experiments (7–14 h).^{31,32}

¹³C DEPT spectra were obtained at 75 °C on a 10% solution of PVB in $\text{Me}_2\text{SO}-d_6$. A total of 16K data points were accumulated over a sweep width of 10 kHz. A total of 400 transients were averaged with a recycle time of 6.8 s. The delay time was set to 3.45 ms, which corresponds to $1/2J$ for a coupling constant of 145 Hz.

The 2D ¹³C-¹H correlated spectrum was obtained on a 10% solution of PVB in $\text{Me}_2\text{SO}-d_6$ at 100 °C. A total of 400 transients were accumulated per t_1 value with a recycle time of 4 s. The initial matrix size was 8065 Hz (2K complex points) and 1800 Hz (128 t_1 values) in ω_2 and ω_1 , respectively. The digital resolution after zero-filling was 3.9 Hz/point and 7.0 Hz/point in ω_2 and ω_1 , respectively, and the total acquisition time was 60 h. The delay times Δ_1 and Δ_2 were set to 3.57 and 1.79 ms, respectively. A sine-bell phase shifted by 45° was used as a filtering function in ω_2 , and a sine-bell with no shift was used in the ω_1 dimension.

The 2D COSY spectrum was obtained on a 5% solution of PVB in $\text{Me}_2\text{SO}-d_6$ at 100 °C. A total of 16 transients were accumulated per t_1 value with a recycle time of 6 s. The initial matrix size was 1800 Hz (1K complex points) in both dimensions, and the digital

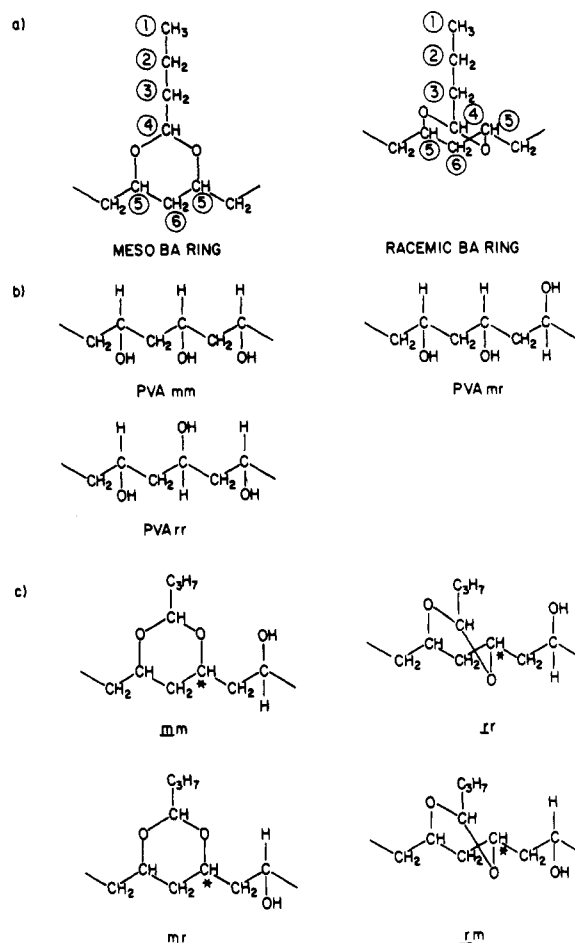


Figure 3. Structures for various stereosequences in PVB. (a) Meso and racemic butyraldehyde rings. The circled numbers are used to identify carbons and protons in the rings. (b) Triad stereosequences associated with poly(vinyl alcohol). (c) Triad stereosequences associated with methine 5 in BA rings. The underlined letter refers to the ring stereochemistry, and the other letter refers to the stereochemistry of the unit adjacent to the ring. An asterisk indicates methine 5 at the center of all sequences.

resolution after zero-filling was 1.8 Hz/point in both dimensions. A sine-bell filtering function was used in both dimensions. The total acquisition time was 14 h.

The 2D J -resolved spectrum was obtained on a 2% solution of PVB in $\text{Me}_2\text{SO}-d_6$ at 100 °C. A total of 64 transients per t_1 value were accumulated with a recycle time of 6 s. The initial matrix size was 2000 Hz (4K complex points) and 62.5 Hz (64 t_1 values) in ω_2 and ω_1 , respectively. The digital resolution after zero-filling was 0.5 Hz/point in both dimensions, and the total acquisition time was 7 h. A sine-bell filtering function was used in both dimensions.

Results and Discussion

Poly(vinylbutyral) is formed when butyraldehyde reacts with adjacent hydroxyls on the poly(vinyl alcohol) chain to form BA rings. The resultant rings are called meso (m) or racemic (r), depending on whether the adjacent hydroxyl groups were in meso or racemic stereochemical configurations in the PVA chain. The structures of meso and racemic BA rings are shown in Figure 3a. Since not all of the hydroxyls react to form BA rings, PVB is essentially a copolymer of BA rings and vinyl alcohol. Due to the large number of possible comonomer sequences and stereosequences in PVB, both the ¹³C and ¹H NMR spectra exhibit complex microstructure.

The ¹³C spectrum of PVB is shown in Figure 4. The multiplicity of each carbon signal can be determined from the series of DEPT spectra shown in Figure 5. The top trace contains all protonated carbon resonances, the middle

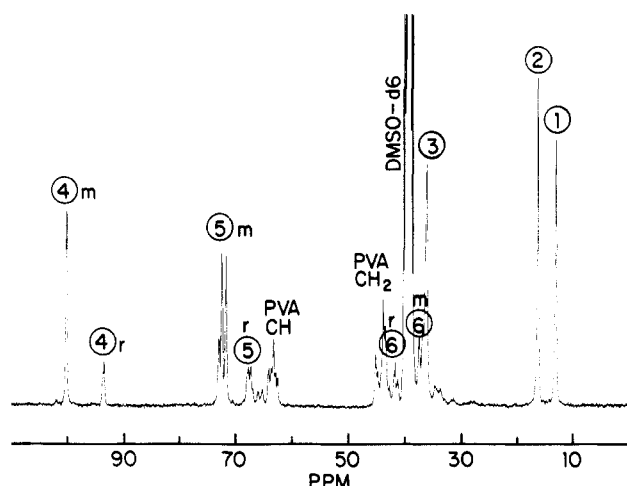


Figure 4. 75-MHz ^{13}C NMR spectrum of a 5% solution of PVB in $\text{Me}_2\text{DSO}-d_6$. The spectrum was obtained with broad-band proton decoupling at a temperature of 100 $^\circ\text{C}$. A total of 2400 transients were recorded with approximately a 65 $^\circ$ pulse and a 10-s relaxation delay. Line broadening of 2 Hz was employed in Fourier transformation of 32K complex points. Labeling refers to Figure 3.

trace contains methine carbon signals only, and the bottom trace has positive signals for methine and methyl resonances and negative signals for methylene resonances. These spectra show that the BA methyl corresponds to the resonance at 13 ppm. Furthermore, all resonances in the range 15–50 ppm are methylenes, and all resonances from 60 to 110 ppm are methines.

More detailed assignments can be made by examining the ^{13}C chemical shifts. The ^{13}C assignments of PVA have been made previously by Ovenall³³ and Tonelli.³⁴ PVA methine resonances exhibit pentad stereosequence microstructure (64–68 ppm), and methylene resonances show tetrad sensitivity in the range 44–46 ppm. Hence, the upfield methine resonances (62–66 ppm) in the ^{13}C spectrum of PVB are assigned as PVA methines, and the downfield methylene resonances (43–46 ppm) are assigned as PVA methylenes. However, the microstructure cannot be assigned in detail to specific stereosequences and/or comonomer sequences.

The BA ring carbons (1–6 in Figure 3) also can be assigned on the basis of chemical shifts. Methylenes 2 and 3 correspond to single lines at 16 and 36 ppm, respectively. No sequence effects are expected or observed for these carbons. However, methine 4 can be part of a meso or racemic ring, and these two rings have different chemical shifts. Regardless of the stereochemistry, this methine is expected to be shifted farther downfield than any other resonance since it is directly attached to two oxygens. Although two stereochemistries are possible for BA rings, meso rings are sterically favored since they are less strained. Therefore, the resonances at 100 and 94 ppm are assigned to methine 4 in meso and racemic rings, respectively. Methine 5 is shifted upfield from methine 4 but downfield from PVA methines since it is in the α -position to an OR group instead of an OH group. Furthermore, two methine 5 carbons exist for each methine 4 carbon. Integration of a ^{13}C spectrum obtained under quantitative conditions (suppressed nuclear Overhauser effect, long relaxation delay, etc.) indicates that methine 5 carbons in meso rings correspond to the three resonances from 72 to 73 ppm. Similarly, methine 5 in racemic rings corresponds to the complex pattern of lines from 67 to 68 ppm. Although the fine structure cannot be assigned unambiguously, it clearly reflects sensitivity to longer sequences. One

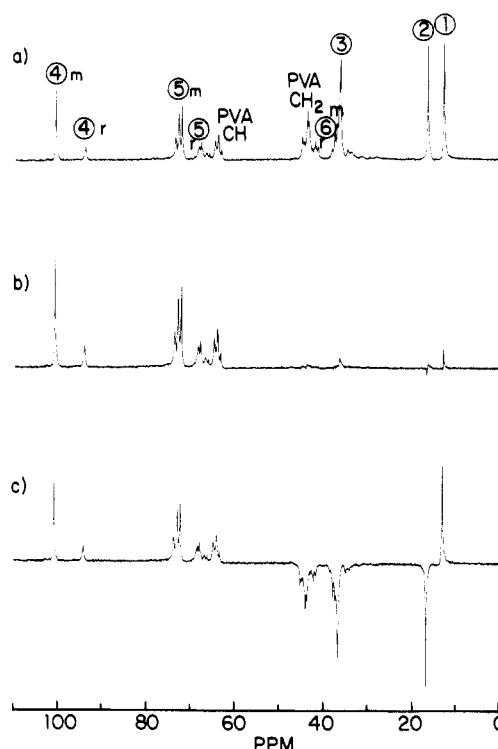


Figure 5. 75-MHz DEPT spectra of PVB: (a) $\theta = 45^\circ$ (all protonated carbons are positive, but quaternary carbons are nulled); (b) $\theta = 90^\circ$ (only methine carbons are present; all other types of carbon signals are nulled); (c) $\theta = 135^\circ$ (methine and methyl carbon signals are positive, but methylene carbons are negative; quaternary carbons have zero intensity).

possible interpretation is that the fine structure associated with methine 5 represents partial resolution of pentad stereosequences. Comparison to the methine region of PVA indicates that mm-centered sequences correspond to resonances that are more downfield from mr and rr sequences. Furthermore, steric considerations indicate that the monomer unit adjacent to a meso ring is more likely to be racemic relative to methine 5 in the ring. Therefore, the fine structure associated with methine 5 is tentatively assigned to mm-, mr-, rm-, and rr-centered sequences in order of increasing field. In this notation, *m* and *r* refer to the orientation of the ring, but *m* and *r* refer to the orientation of neighboring monomer units as shown in Figure 3c. In contrast to methine 5, which is shifted downfield from PVA methines, methylene 6 is shifted upfield relative to PVA methylenes. More specific assignments will be discussed below.

The line assignments for the ^{13}C spectrum are transferred to the proton spectrum by 2D ^{13}C – ^1H correlated spectroscopy. The 2D ^{13}C – ^1H correlated spectrum is a map of each ^{13}C resonance to the corresponding proton resonances of all directly attached protons. The proton assignments made from this map can be verified by the proton COSY spectrum, which is a map of ^1H – ^1H couplings.

The ^1H spectrum of PVB at 100 $^\circ\text{C}$ is shown in Figure 6, and the 2D ^{13}C – ^1H correlated spectrum is shown in Figure 7. Methine 4 protons in meso and racemic rings correspond to the two downfield resonances at 4.5 and 4.8 ppm, respectively, since the methine 4 carbon resonances map to these proton resonances in the 2D ^{13}C – ^1H correlated spectrum. Similarly, PVA methine protons correspond to resonances in between resonances for methine 5 BA ring protons in racemic (4.2 ppm) and meso (3.8 ppm) rings. Somewhere in this region are resonances corresponding to PVA hydroxyl protons, but these cannot be

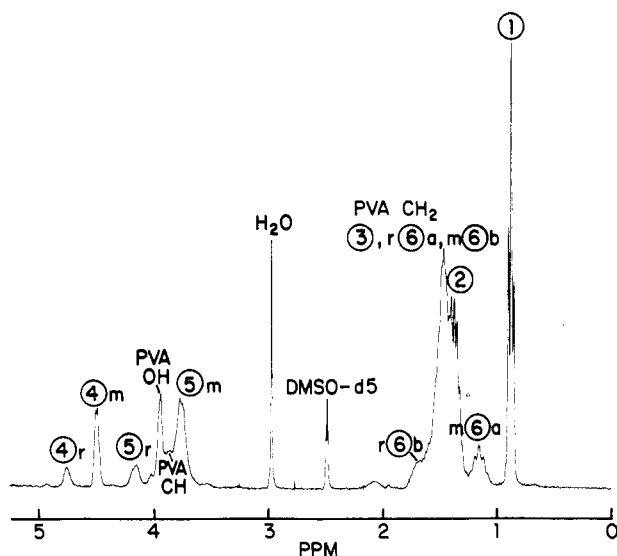


Figure 6. 300-MHz ^1H NMR spectrum of a 2% solution of PVB in $\text{Me}_2\text{SO}-d_6$ at a temperature of 100 $^\circ\text{C}$. A total of 32 transients were recorded with a 90° pulse and a 10-s recycle time using 16K complex data points. Labeling refers to Figure 3.

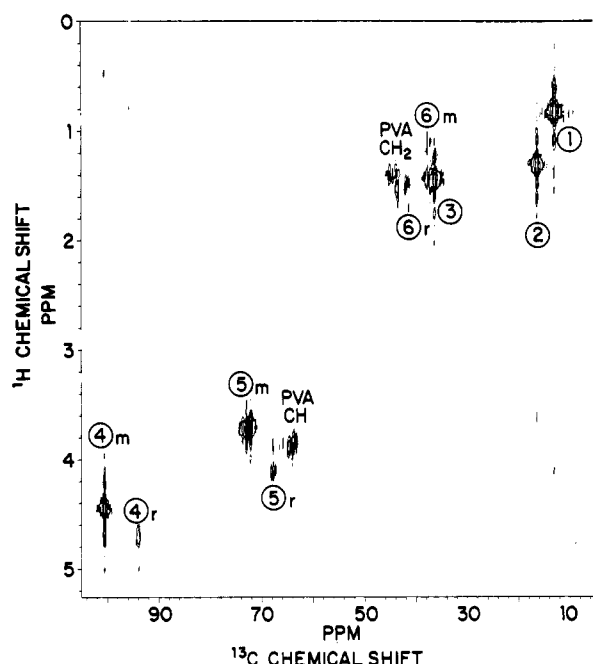


Figure 7. 2D ^{13}C - ^1H correlated spectrum of PVB at 100 $^\circ\text{C}$. The ^{13}C chemical shift of each peak is indicated on the horizontal axis, and the corresponding ^1H chemical shifts of all directly attached protons is indicated on the vertical axis.

identified from the ^{13}C - ^1H spectrum since hydroxyl protons have no directly attached carbons. The lack of observable cross peaks in the COSY spectrum due to J -coupling between PVA methine and hydroxyl protons indicates that the hydroxyl resonances are overlapped with PVA methine resonances. This will be discussed in more detail later.

The carbon resonance corresponding to methyl 1 maps to the upfield triplet (split by neighboring methylene 2 protons) in the proton spectrum. Hence, this triplet at 0.9 ppm is assigned to the BA methyl 1 protons. The methylene protons can be assigned from the methylene region of the ^{13}C - ^1H correlated spectrum. This spectrum indicates that each of the two pairs of methylenes, 2 and 3, are equivalent and that methylene 2 has a proton resonance upfield from methylene 3. However, the carbon resonance for methylene 6 in meso rings maps to two

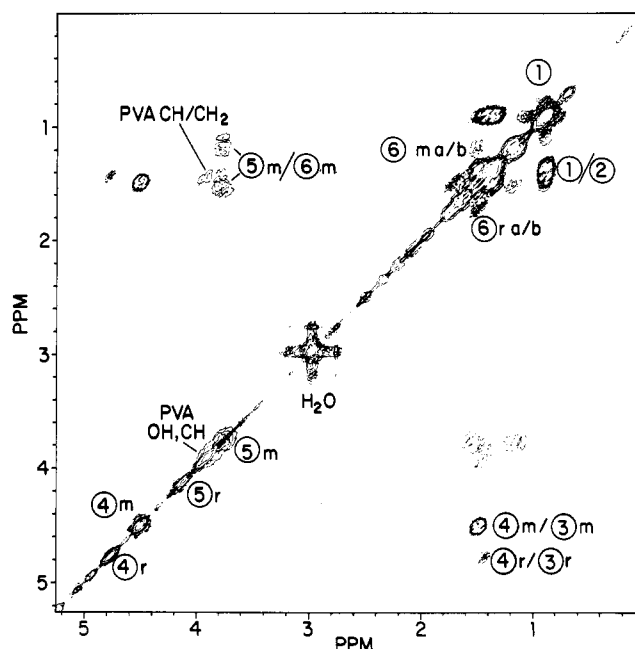


Figure 8. 300-MHz 2D homonuclear correlated (COSY) spectrum of PVB at 100 $^\circ\text{C}$. The normal spectrum is contained along the diagonal, and cross peaks connect protons which are J -coupled.

nonequivalent methylene 6 resonances, and the proton resonances at 1.5 and 1.2 ppm are assigned to these nonequivalent methylenes. Similarly, the carbon resonance for methylene 6 in racemic rings maps to two nonequivalent protons at 1.7 and 1.5 ppm. The PVA methylene protons are identified by the cross peaks corresponding to the PVA carbon methylenes. As in the methine region, the PVA methylene protons have ^1H chemical shifts in between the average chemical shift of the nonequivalent methylene 6 protons in racemic and meso rings. Fine structure due to stereosequences is observed in the ^{13}C - ^1H correlated spectrum. Furthermore, differences in degrees of nonequivalence are observed for pairs of methylenes in the center of different sequences. The m-centered PVA methylene carbons are upfield from the r-centered, and the m-centered show a greater ^1H chemical shift difference between methylene protons than do the r-centered as expected.

The ^1H assignments made from the 2D ^{13}C - ^1H correlated spectrum are verified by the proton J -couplings observed in the COSY spectrum shown in Figure 8. Coupling is observed between methine and methylene protons in PVA and between backbone methine 5 and methylene 6 in BA rings. J -coupling is also observed along the BA side chain between methyl 1 and methylene 2, methylene 2 and methylene 3, and methylene 3 and methine 4. The better signal-to-noise ratio and resolution of the COSY experiment allow more accurate measurement of the chemical shifts of the methylene protons. For instance, cross peaks connecting methine 4 and methylene 3 show that the two methylene 3 protons are indeed equivalent, but methylene 3 protons in a racemic ring are shifted slightly upfield relative to these protons in a meso ring. The cross peak from BA methyl 1 to methylene 2 pinpoints the location of methylene 2 slightly upfield of methylene 3, in agreement with that observed in the ^{13}C - ^1H correlated spectrum. Cross peaks connecting BA methylenes 2 and 3 are also observed. In the methine region, the upfield resonance corresponding to methine 5 in a meso ring shows cross peaks to two nonequivalent methylene 6 protons at the same chemical shifts observed in the ^{13}C - ^1H correlated spectrum. Furthermore, cross peaks corresponding to the

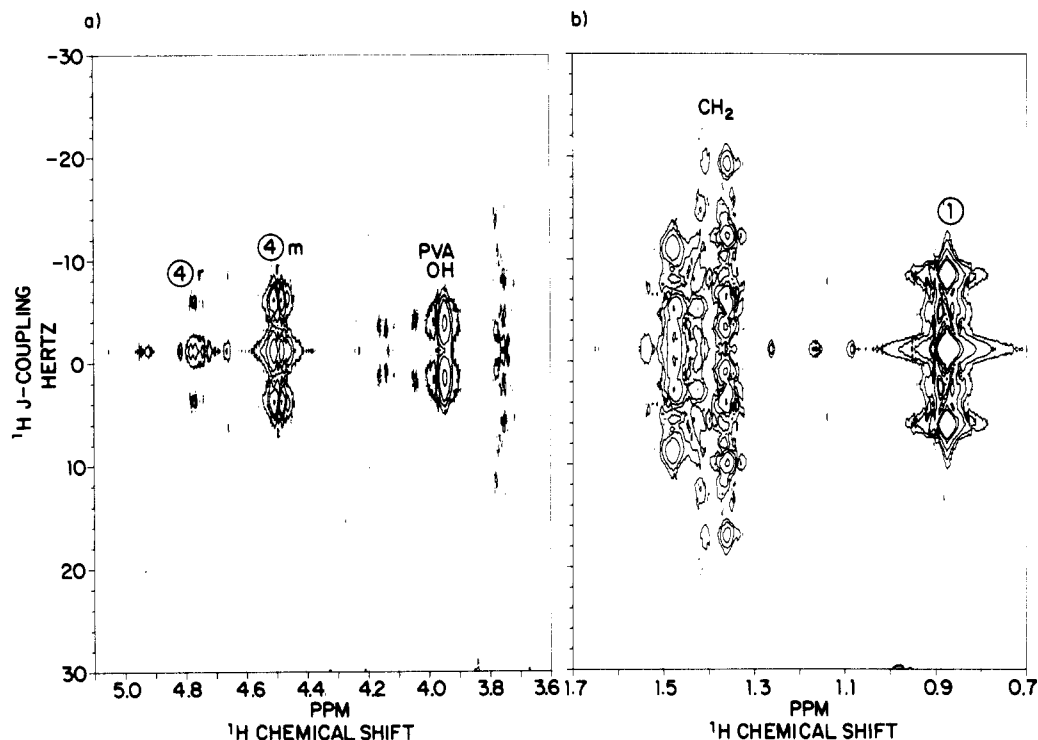


Figure 9. 300-MHz 2D J -resolved spectrum of PVB at 100 °C. The ^1H chemical shift is indicated along the horizontal axis, and the J -coupling is indicated along the vertical axis: (a) expansion of CH,OH region of spectrum; (b) expansion of CH_2, CH_3 region of spectrum.

geminal coupling between these two nonequivalent methylenes are observed. PVA methylenes are identified from methine/methylene cross peaks. As observed in the ^{13}C - ^1H correlated spectrum, the PVA methylene protons have chemical shifts near the middle of the methylene region. There should be cross peaks connecting methine 5 to two nonequivalent methylenes 6 in a racemic ring, but no cross peaks are observed. There are cross peaks observed for the geminal coupling between these methylene protons, and these cross peaks verify the assignments made from the ^{13}C - ^1H correlated spectrum. The missing cross peaks are probably absent due to short spin-spin relaxation times (T_2) of these protons. At room temperature, no backbone methine/methylene cross peaks are observed in the COSY spectrum; cross peaks in this region are only observed upon heating to 100 °C. This indicates that the T_2 values are quite short for the backbone protons. Hence, the weak signal associated with the low-abundance racemic rings probably is lost due to spin-spin relaxation during the time interval t_1 . Aside from these missing cross peaks, the assignments made from the ^{13}C - ^1H correlated experiment are verified by the COSY results. The results are summarized in Table I.

Now that the ^1H line assignments are established, proton coupling constants can be measured from the 2D J -resolved spectrum shown in Figure 9. The methine region is expanded on the left and the methylene and methyl region is expanded on the right. Triplets are observed for BA methine 4 in racemic and meso rings as expected. Furthermore, at least three chemical shifts are observed for both racemic and meso methine 4, and all six chemical shift have the same coupling constant of approximately 5 Hz. This fine structure must be due to sensitivity to longer sequences. One interpretation is that these six triplets correspond to the six tetrad stereosequences containing meso and racemic rings given by rrr , mrr , rrm , rmr , rmm , and mmm . Steric considerations indicate that a meso unit adjacent to a meso ring is unlikely due to crowding. Hence, the three m -centered triplets are assigned to rmr , rmm , and mmm in increasing field on the

Table I
Chemical Shifts and Homonuclear Coupling Constants for PVB in $\text{Me}_2\text{SO}-d_6$ at 100 °C

assignment ^a	^{13}C chem shift, ^b ppm	^1H chem shift, ^c ppm	homonuclear coupling constant, ^d Hz
meso BA CH 4	100.2	4.51, 4.49, 4.47	5.0
rac BA CH 4	93.5	4.79, 4.77, 4.75	4.9
meso CH 5	73.1, 72.5, 71.8	3.77	<i>e</i>
rac CH 5	68.1–67.3	4.15	<i>e</i>
PVA CH	65.5–62.2	3.91	<i>e</i>
PVA CH_2	45.4–42.8	1.44	<i>e</i>
rac CH_2 6:a	42.0, 41.4	1.50	<i>e</i>
rac CH_2 6:b	42.0, 41.4	1.71	<i>e</i>
meso CH_2 6:a	37.7, 36.9	1.16	<i>e</i>
meso CH_2 6:b	37.7, 36.9	1.48	<i>e</i>
meso BA CH_2 3	36.2	1.48	<i>e</i>
rac BA CH_2 3	36.2	1.41	<i>e</i>
BA CH_2 2	16.4	1.38	<i>e</i>
BA CH_3 1	13.2	0.88	7.4
mm PVA OH		4.05	6.1
mr PVA OH		3.99	5.8
rr PVA OH		3.95	5.5

^a Assignments refer to Figure 3. For nonequivalent methylene protons, the two protons are designated as a and b. ^b Referenced to 39.5 ppm for $\text{Me}_2\text{SO}-d_6$. Uncertainty limits are ± 0.1 ppm. ^c Referenced to 2.49 ppm for $\text{Me}_2\text{SO}-d_6$. Uncertainty is ± 0.03 ppm. ^d Coupling constants measured from 2D J -resolved spectrum. Uncertainty is ± 0.2 Hz. ^e Coupling constants were not measured due to complexity of coupling pattern.

basis of their relative intensities. The backbone methines are not clearly observed in the 2D J -resolved spectrum due to the complex coupling patterns and short T_2 associated with these protons. However, three doublets corresponding to PVA hydroxyl protons are observed at 4.05, 4.0, and 3.95 ppm. Since the PVA portion of PVB is depleted in meso diads, the hydroxyl doublets are assigned to mm , mr , and rr triads in order of increasing field on the basis of the relative intensities observed in the J -resolved spectrum. Hence, the 2D J -resolved spectrum allows the hydroxyl chemical shifts to be determined. As expected, the hydroxyl protons are overlapped with PVA methine protons.

Furthermore, the PVA CH/OH coupling constants are found to vary somewhat with stereosequence, ranging from 6.1 Hz in mm sequences to 5.5 Hz in rr sequences. This indicates that the average CH–OH dihedral angle varies somewhat with the stereosequence for PVA sequences in PVB. The methylene region of the 2D *J*-resolved spectrum shows an extremely complex pattern of lines which cannot be readily interpreted due to complications from strong coupling. The BA methyl 1 shows a single triplet with a coupling constant of 7.4 Hz. The coupling constants measured from the 2D *J*-resolved spectrum are summarized in Table I.

Conclusions

Line assignments in the ¹³C spectrum of PVB are made from DEPT spectra, chemical shifts and relative intensities. The proton assignments obtained from the ¹³C–¹H correlated spectrum are transferred to the proton spectrum by 2D ¹³C–¹H correlated spectroscopy. These assignments are confirmed by the COSY spectrum. Furthermore, ¹H chemical shifts can be accurately measured from the COSY spectrum despite severe overlap of resonances in the normal spectrum. Once the assignments are known, coupling constants for some of the protons can be measured from the 2D *J*-resolved spectrum. Furthermore, longer sequences can be observed in the 2D *J*-resolved spectrum. The BA 4/3 coupling constant does not change with the stereochemistry, indicating that the average CH/CH₂ dihedral angle of the BA side chain does not vary with the stereosequence. However, slight changes in the CH/OH coupling constant are observed in different PVA stereosequences in PVB. This indicates slight sequence-dependent variation in the backbone chain conformation.

The combination of several modern NMR techniques allows detailed assignments to be made in the ¹³C and ¹H spectra of an extremely complex polymer. Furthermore, scalar coupling constants can be measured from the 2D *J*-resolved spectrum which cannot be obtained otherwise. The combination of high-field and modern NMR techniques shows much promise for interpretation of ¹H spectra of complex polymers.

References and Notes

- (1) Kumar, A.; Wagner, G.; Ernst, R. R.; Wüthrich, K. *Biochem. Biophys. Res. Commun.* **1980**, *96*, 1156.
- (2) Nagayama, K.; Wüthrich, K. *Eur. J. Biochem.* **1981**, *114*, 365.
- (3) Nagayama, K.; Wüthrich, K.; Bachmann, P.; Ernst, R. R. *Biochem. Biophys. Res. Commun.* **1977**, *78*, 99.
- (4) Wüthrich, K.; Wider, G.; Wagner, G.; Braun, W. *J. Mol. Biol.* **1982**, *155*, 311.
- (5) Wider, G.; Lee, K. H.; Wüthrich, K. *J. Mol. Biol.* **1982**, *155*, 367.
- (6) Arseniev, A. S.; Wider, G.; Joubert, F. J.; Wüthrich, K. *J. Mol. Biol.* **1982**, *159*, 323.
- (7) Rance, M.; Wagner, G.; Sørensen, O. W.; Wüthrich, K.; Ernst, R. R. *J. Magn. Reson.* **1984**, *59*, 250.
- (8) Haasnoot, C. A. G.; Pandit, U. K.; Kruk, C.; Hilbers, C. W. *J. Biomolec. Struct. Dyn.* **1984**, *2*, 449.
- (9) Kessler, H.; Hehlein, W.; Schuck, R. *J. Am. Chem. Soc.* **1982**, *104*, 4534.
- (10) Davoust, D.; Bodo, B.; Rebuffat, S.; Platzer, N. *Biochem. Biophys. Res. Commun.* **1983**, *116*, 1.
- (11) Nygaard, E.; Mendz, G. L.; Moore, W. J.; Martenson, R. E. *Biochemistry* **1984**, *23*, 4003.
- (12) Koizuka, I.; Watari, H.; Yanaihara, N.; Nishina, Y.; Shiga, K. *Biomed. Res.* **1984**, *5*, 161.
- (13) Bruch, M. D.; Noggle, J. H.; Gierasch, L. M. *J. Am. Chem. Soc.* **1985**, *107*, 1400.
- (14) Kan, L. S.; Cheng, D. M.; Cadet, J. *J. Magn. Reson.* **1982**, *48*, 86.
- (15) Weiss, M. A.; Patel, D. J.; Sauer, R. T.; Karplus, J. *Am. Chem. Soc.* **1984**, *106*, 4269.
- (16) Hall, L. D.; Morris, G. A.; Sukumar, S. *Carbohydr. Res.* **1979**, *76*, C7.
- (17) Dabrowski, J.; Hanfland, P. *FEBS Lett.* **1982**, *142*, 138.
- (18) Bruch, R. C.; Bruch, M. D. *J. Biol. Chem.* **1982**, *257*, 3409.
- (19) Bruch, M. D.; Bovey, F. A.; Cais, R. E.; Noggle, J. H. *Macromolecules* **1985**, *18*, 1253.
- (20) Macura, S.; Brown, L. R. *J. Magn. Reson.* **1983**, *53*, 529.
- (21) Brown, L. R. *J. Magn. Reson.* **1984**, *57*, 513.
- (22) Gippert, G. P.; Brown, L. R. *Polym. Bull.* **1984**, *11*, 585.
- (23) Schilling, F. C.; Bovey, F. A.; Bruch, M. D.; Kozlowski, S. A. *Macromolecules* **1985**, *18*, 1418.
- (24) Cheng, H. N.; Lee, G. H. *Polym. Bull.* **1984**, *12*, 463.
- (25) Cheng, H. N.; Lee, G. H. *Polym. Bull.* **1985**, *13*, 549.
- (26) Doddrell, D. M.; Pegg, D. T.; Bendall, M. R. *J. Magn. Reson.* **1982**, *48*, 323.
- (27) Bendall, M. R.; Pegg, D. T.; Doddrell, D. M. *J. Magn. Reson.* **1981**, *45*, 8.
- (28) Nagayama, K.; Kumar, A.; Wüthrich, K.; Ernst, R. R. *J. Magn. Reson.* **1980**, *40*, 321.
- (29) Aue, W. P.; Karhan, J.; Ernst, R. R. *J. Chem. Phys.* **1976**, *64*, 4226.
- (30) Brownstein, S. *J. Magn. Reson.* **1981**, *42*, 150.
- (31) Bauman, R.; Wider, G.; Ernst, R. R.; Wüthrich, K. *J. Magn. Reson.* **1981**, *44*, 402.
- (32) Mersh, J. D.; Sanders, J. K. M. *J. Magn. Reson.* **1982**, *50*, 171.
- (33) Ovenall, D. W. *Macromolecules* **1984**, *17*, 1458.
- (34) Tonelli, A. E. *Macromolecules* **1985**, *18*, 1086.